

Performance of a geocomposite liner for containing Jet A-1 spill in an extreme environment[☆]

R.K. Rowe^{a,*}, T. Mukunoki^b, R.J. Bathurst^c, S. Rimal^a, P. Hurst^a, S. Hansen^a

^a*GeoEngineering Centre at Queen's-RMC, Queen's University, Kingston, Ont., Canada K7L 3N6*

^b*Department of Civil and Environmental Engineering, Kumamoto University, Kumamoto, Japan*

^c*GeoEngineering Centre at Queen's-RMC, Royal Military College, Kingston, Ont., Canada K7K 7B4*

Received 22 May 2005; received in revised form 1 September 2006; accepted 16 October 2006

Available online 22 January 2007

Abstract

A composite liner comprised of a fluorinated high-density polyethylene (f-HDPE) geomembrane and geosynthetic clay liner (GCL) was used to contain a hydrocarbon spill in the Canadian Arctic. Results of laboratory tests conducted to assess the effect of exposure to cold climates and hydrocarbons on the performance of the GCL and f-HDPE geomembrane with time are reported herein. The effect of freeze–thaw conditions on the short-term low-gradient and the long-term high-gradient hydraulic conductivity of unfrozen GCL specimens is examined with respect to permeation by Arctic diesel (jet fuel). The hydraulic conductivity of frozen GCL specimens is also discussed. The effect of contact with jet fuel on the chemical and mechanical properties of the geomembrane is reported. Finally, the implications of these extreme conditions on the likely performance of the composite liner are discussed.

© 2006 Elsevier Ltd. All rights reserved.

Keywords: GCL; Freeze–thaw; Geomembrane; Hydrocarbons; Hydraulic conductivity; Ageing

1. Introduction

There has been considerable progress in terms of researching the performance of composite liners and their geosynthetic components over the past few years (e.g. Rowe and Orsini, 2003; Cartaud et al., 2005a, b; Lake and Rowe, 2005; Rowe, 2005; Barroso et al., 2006; Bouazza and Vangpaisal, 2006; Touze-Foltz et al., 2006; Dickinson and Brachman, 2006) however to-date there has been very little research relating to the use of composite liners in extreme climates. Brevoort Island (located in northern Canada near Baffin Island) is a former Pole Vault radar early warning site where it has been necessary to contain spills and leaks of Arctic diesel (jet fuel) prior to possible future remedia-

tion. At this site permafrost, which is located at a relatively shallow depth, provides a natural barrier to prevent significant downward migration of hydrocarbons. However, the shallow permafrost layer also contributes to lateral spreading of the hydrocarbon plume, particularly following infiltration by rainwater and snow melt. A cleanup programme has been initiated by the Canadian Department of National Defence. However, because of the difficulties of site access and the very short construction season, it has been necessary to provide “short-term” containment to allow time for more permanent measures to be implemented. A novel geosynthetic composite barrier system was used to provide this containment (Bathurst et al., 2006). The system comprised (from bottom up) a needle-punched geosynthetic clay liner (GCL), a fluorinated high-density polyethylene (f-HDPE) geomembrane, a needle-punched geotextile protection layer which was constructed on the down-gradient slope of a trench excavated to permafrost during the summer of 2001 (Li et al., 2002). The area above the plume was covered with a geomembrane and the surface graded to minimize infiltration of rainwater or runoff into the contaminated zone.

[☆]This paper is a modified and expanded version of a paper by Rowe et al. (2005b) initially presented at the ASCE Geo-Frontiers 2005 Conference, Austin, January 2005. Any material from this earlier paper is reproduced here with the permission of the ASCE.

*Corresponding author. Tel.: +1 613 533 6933; fax: +1 613 533 6934.

E-mail addresses: kerry@civil.queensu.ca (R.K. Rowe), mukunoki@kumamoto-u.ac.jp (T. Mukunoki), bathurst-r@rmc.ca (R.J. Bathurst).

Given the novel, and experimental, nature of the barrier combined with the extreme environmental conditions at Brevoort Island, a laboratory and field monitoring programme were initiated to provide insight regarding how long the “temporary” liner might be expected to provide an adequate barrier to the hydrocarbon plume. The objective of this paper is to summarize findings from these studies to date. Consideration is given to the effects of: (a) the interaction between jet fuel and both the geomembrane and GCL; (b) freeze–thaw on the hydraulic conductivity of the GCL; and (c) unsaturated conditions on the hydraulic conductivity of the GCL with respect to jet fuel for both frozen and unfrozen conditions. Since jet fuel is an organic immiscible liquid, the following effects are considered when examining GCL performance: (1) the water–jet fuel interface in the soil pores; (2) the interaction between jet fuel and the bentonite double layer; and (3) changes in pore structure of bentonite due to freeze–thaw and permeation by jet fuel. The effect of the choice of test method on laboratory results is also examined. Finally, specimens from two different HDPE geomembrane materials (a conventional untreated product and an especially fluorinated geomembrane used in the field barrier) were exposed to jet fuel and the effect on both the tensile properties and the oxidative induction time (OIT) were assessed with respect to immersion time.

2. Test methods and materials

2.1. Procedure for hydraulic conductivity tests

Tables 1 and 2 give the basic properties of the GCL used in the current investigation and permeants (de-aired water and jet fuel) tested. The thermally treated, needle-punched GCL consisted of a uniform layer of granular sodium bentonite encapsulated between a scrim-reinforced non-woven polypropylene carrier and a staple fibre nonwoven polypropylene cover geotextile. The average mass per unit area of the cover and carrier geotextiles, and bentonite were 250, 270 and 3800 g/m², respectively. Tests were performed using both rigid wall (RWP) and flexible wall (FWP) permeameters. Each has advantages and disadvantages. The RWP (see Fernandez and Quigley (1985) or

Rowe et al (2004a) or Rowe et al. (2005a, b) for details and a schematic drawing) has a specified flow (with the pressure being measured and the gradient deduced). This test has the advantage that large pore volumes of permeant can be passed through the GCL in a reasonable period of time, allowing tests to be readily run to chemical equilibrium. However it also means that the gradients are very high and are usually many orders of magnitude great than field gradients. In some cases this may mean that the hydraulic conductivity deduced from the test is not representative of field conditions (as discussed later). The FWP has a specified gradient and the corresponding flow is measured. This allows small gradients, representative of field conditions, to be applied; however it may take many months, to years to reach chemical equilibrium under low gradients. Both tests were used in this study to take advantage of the strength of each test and also to identify the implications of test method on the deduced hydraulic conductivity with respect to jet fuel. The issues of side wall leakage and a comparison of different methods of performing hydraulic conductivity tests on GCLs has been discussed by Petrov et al. (1997) and the interested reader is referred to that paper for more details. Specimens were inspected following each test in the RWP to identify if there was any evidence of side wall leakage. No side wall leakage was observed.

GCL specimens were prepared in the same way for both RWP and FWP tests, and in each case the specimens were:

- (1) hydrated (from the bottom) for 5 days under a confining pressure of about 14 kPa at an hydraulic gradient of 20;
- (2) subjected to 0, 5 or 12 freeze–thaw cycles;
- (3) permeated with de-aired water to establish the reference hydraulic conductivity (k) with respect to water; and then,
- (4) permeated with jet fuel to establish the hydraulic conductivity with respect to jet fuel.

For the hydraulic conductivity tests using an unsaturated GCL specimen, step 3 was omitted.

2.2. Rigid wall permeameter (RWP) tests

A 54 mm (internal diameter) rigid wall permeameter, similar to that used by Petrov and Rowe (1997), was used to assess the hydraulic conductivity of the GCL after permeation by many pore volumes of permeant at an influent flow rate of 3.18 mL/day. A stress of 12–18 kPa was applied to the GCL specimen by springs acting on a porous plate. A dial gauge was attached to a plate on the GCL specimen and the thickness of GCL was monitored during hydration and permeation of the specimen. The influent pressure and effluent flow rate were monitored during permeation, and the hydraulic conductivity was calculated from this data using Darcy’s Law. Unless otherwise noted, the test temperature was 20 ± 1 °C.

Table 1
Characteristics of GCL material tested

	Test method	Mass per unit area	
		Specified values (g/m ²)	Measured values (g/m ²)
Cover and carrier geotextile	ASTM D 5261 (1992)	200 MARV ^a	250 (SD ^b : 26) 270 (SD ^b : 13)
Mass per unit area of bentonite	ASTM D 5993 (1996)	3660 MARV ^a	3, 800 (SD ^b : 260)

^aMinimum average roll value.

^bStandard deviation.

Table 2
Density and dynamic viscosity of de-aired water and jet fuel

Temperature (°C)	De-aired water		Jet fuel	
	Density ^a (g/cm ³)	Dynamic viscosity ^a (MPa-s)	Relative density	Dynamic viscosity (MPa-s)
-20	0.9168 ^b	—	< 0.91 ^c	7.28 ^e
-5	0.9168 ^b	—	0.85 ^d	5.65 ^f
5	0.9999	1.52	0.83 ^c	3.88 ^f
20	0.9977	0.98	0.82 ^c	2.76 ^f

^aASTM D1480-91, 1998b.

^bElert (2003).

^cMeasured values based on ASTM D1480-91, 1998b.

^dDeduced values from trend curve based on relative density measured (i.e. value with superscript c).

^eDeduced values from the relative density at -20 °C and kinematic viscosity given by CHEM INFO (2001–2002).

^fDeduced values from equation obtained from Lewis and Squires (1934)

To provide insight into the behaviour of unsaturated GCLs permeated with jet fuel, GCL specimens initially hydrated to different water contents were permeated with jet fuel at four temperatures: 20, 5, -5 and -20 °C. Additional tests were run with specimens that were first permeated with jet fuel at +5 °C and then frozen to -5 °C and permeated again with jet fuel.

2.3. Flexible wall permeameter (FWP) tests

FWP tests were conducted on 70 mm-diameter specimens using a Tri-Flex 2 Permeability Test system (Hoskin Science), with 195 mL pressure interface chambers (model K-790A) to control and monitor jet fuel inflow and outflow. Mukunoki et al. (2003) examined the chemical resistance of the membrane sleeve and reported that both conventional latex and neoprene sleeves do not work well. In this test, a viton membrane sleeve was used and found to perform well (i.e. no evident chemical interaction over 6 months of jet fuel permeation). The hydraulic conductivity was evaluated based on ASTM D5084-90 (1997) and ASTM D6766-02 (2002) methods of test.

2.4. Freeze-thaw cycle tests

After hydration, the entire RWP cell was placed in a freezer at -15 °C. After about 24 h, the cell was placed in a room with a regulated temperature of 22 ± 1 °C for about 24 h (ASTM D6035-96, 1997). This procedure was repeated 5 and 12 times. There was no additional supply of water to the GCL specimen during the freeze-thaw cycles.

The conventional FWP cell is too large to place the entire cell in the freezer. Thus a special chamber was developed to hydrate a GCL specimen and subject it to freeze-thaw cycles as shown in Fig. 1. The freeze-thaw cycles were applied as described above for the RWP specimens. After completion of the last freezing, the GCL specimens were removed from the chamber and installed into the FWP, and the last thaw cycle was completed in the FWP cell. This procedure minimized the effect of stress

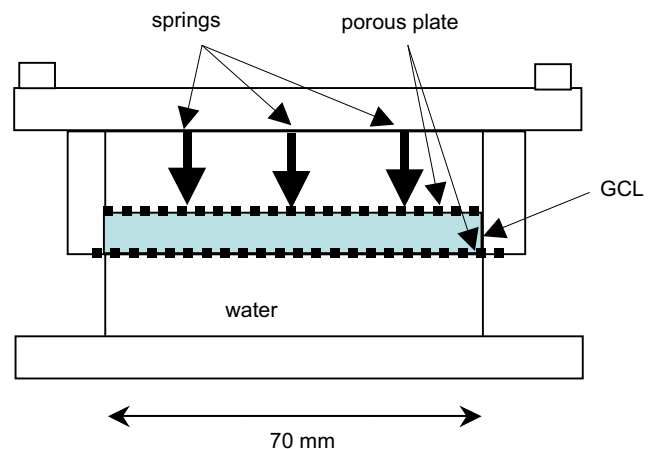


Fig. 1. Schematic of freeze-thaw cell for a flexible wall permeability test.

release when the specimen was transferred from the special chamber to the FWP because the frozen specimen did not experience any significant volume change during the transfer.

2.5. Geomembrane properties

The untreated HDPE geomembrane was manufactured by GSE Lining Technology Inc., Houston, Texas, USA. This 1.5 mm-thick (60 mil), smooth black-surfaced f-HDPE geomembrane is produced from specially formulated virgin polyethylene resin. The average density of the geomembrane is 0.94 g/cm³. As per manufacturers' information it contains approximately 97.5% polyethylene and the remaining 2.5% consists of carbon black, trace amounts of antioxidants and heat stabilizers. It does not contain any other additives, fillers or extenders. The standard oxidative inductive time (OIT) value for the geomembrane is 135 min. This OIT value is greater than the minimum value of 100 min required by the Ontario Regulation 232/98—Environmental Protection Act, 1998. The thickness of 1.5 mm is the minimum value recommended by Ontario regulations.

The fluorinated f-HDPE geomembrane was first produced as a conventional geomembrane and then fluorinated by exposing the geomembrane to elemental fluorine gas on both sides. In this surface fluorination process, the fluorine atoms substitute for hydrogen atoms in the carbon–hydrogen (C–H) polyethylene chain, creating carbon–fluorine (C–F) covalent bonds on the surface of the untreated geomembrane. This creates a thin carbon–fluorine layer on both sides of the geomembrane. The thickness of the fluorinated layer was measured to be 0.31–0.37 μm using a scanning electron microscope (Energy Dispersive X-ray). The fluorination of HDPE is carried out to improve permeation resistance to hydrocarbons. The relevant properties of both geomembranes are summarized in Table 3.

2.6. Tensile tests

Tensile tests were performed to assess the changes in the mechanical properties of the geomembrane due to exposure to jet fuel. These tests were conducted using a Universal testing machine (Instron Model 3396), a 5 kN load cell, and self-aligning wedge grips suitable for dumbbell-shaped specimens (ASTM D638-97, 1998a for Type IV specimen; and ASTM D6693-01, 2003), and a data acquisition system. The specimens were cut using a standard die. Results (load and elongation at yield and break) were obtained in accordance with ASTM D6693-01 (2003) using specimens tested at a speed of 50 mm/min. The load and elongation data were recorded until the specimen ruptured. Tensile properties at yield and break were evaluated using this data.

2.7. Oxidative induction time (OIT) tests

OIT is considered to be a good indicator of the amount of antioxidant present in the geomembrane. It is extremely useful for monitoring the depletion of antioxidants in the geomembrane (Koerner et al., 1992; Hsuan and Koerner, 1995; Hsuan and Koerner, 1998; Sangam and Rowe, 2002; Müller and Jakob, 2003). Standard OIT tests were conducted using a differential scanning calorimeter (DSC) (TA Instruments DSC 2910) following ASTM

D3895-97 (1998c). In this test, the geomembrane specimen is heated in the DSC cell from room temperature to an elevated temperature of 200 °C at a heating rate of 20 °C/min under nitrogen atmosphere (flow rate of 50 cc/min). Then the gas is switched from inert nitrogen to oxygen under isothermal conditions. The test is completed after the exothermal peak resulting from oxidation is reached (Hsuan and Koerner, 1995). The time from the initial introduction of oxygen to the onset of the exotherm is then reported as the OIT value.

3. Results and discussion

3.1. Assessment of hydraulic performance of GCL specimens

3.1.1. Hydraulic conductivity of GCL specimens subjected to freeze–thaw cycles

Tables 4 and 5 summarize key physical (mass per unit area, void ratio with respect to water and jet fuel permeation, final fluid content) and hydraulic (mean hydraulic conductivities and hydraulic gradients) properties of the GCL specimens; obtained from both the RWP and FWP tests. In Table 4, the subscripts ‘w’, ‘j’ and ‘B’, denote ‘entire effluent is water’, ‘entire effluent is jet fuel’, and ‘bulk void ratio’, respectively. There were three stages to both the RWP and FWP tests. In stage 1, de-aired water was permeated through the GCL. In stage 2, jet fuel was permeated through the GCL but the effluent at this stage

Table 4
Physical properties of GCL used for hydraulic conductivity tests

Test method	Number of freeze–thaw cycles	M_{GCL} (g/m ²)	e_{Bw}	e_{Bj}	Fluid content L^{c} (%)
RWP	0	4464	4.3 ^a	3.6	133
RWP	5	4247	6.3 ^a	5.8	192
FWP	0	4316	4.2 ^b	3.9	144
FWP	12	4451	5.6 ^b	5.2	226

^aAt the end of water permeation.

^bBefore water permeation.

^c $L = M_{\text{L}}/M_{\text{s}}$, where M_{L} is a mass of fluid in the bentonite and M_{s} is dry mass of bentonite.

Table 3
Properties of the geomembranes examined

Property	Method	Untreated		Fluorinated	
		Average	COV	Average	COV
Thickness (mm)	As received	1.5	—	1.5	—
OIT (min)	ASTM D3895 (1998c)	135	1.5	137	0.7
Crystallinity (%)	ASTM E794 (1998d)	52	2.4	51	2.2
Tensile strength at yield (kN/m)	ASTM D6693 (2003)	24	3.7	23	2.4
Tensile strength at break (kN/m)	ASTM D6693 (2003)	51	10.5	54	2.5
Tensile strain at yield (%)	ASTM D6693 (2003)	20	1.9	20	2.8
Tensile strain at break (%)	ASTM D6693 (2003)	869	11.9	979	2.8

COV = coefficient of variation; OIT = oxidative induction time.

Table 5
Hydraulic conductivity and hydraulic gradient of GCL specimens with respect to both water and jet fuel

Test method	Hydraulic conductivity (m/s)				Hydraulic gradient (–)		
	k_1	k_2	k_3	k_3/k_1	i_1	i_2	i_3
RWP (0) ^a	2.0×10^{-11}	8.2×10^{-12}	2.0×10^{-11}	1	730	1153	723
RWP (5) ^a	2.0×10^{-11}	5.8×10^{-12}	8.0×10^{-11}	4	750	790	222
FWP (0) ^a	3.4×10^{-11}	6.2×10^{-13}	4.0×10^{-11}	1.2	83	381	685
FWP (12) ^a	4.1×10^{-11}	2.4×10^{-12}	6.0×10^{-11}	1.5	45	159	313

^a()Number of freeze-thaw cycles.

was a mixture of both pore water and jet fuel. In stage 3, the effluent was entirely jet fuel. The hydraulic conductivities (k_1 , k_2 , k_3), and hydraulic gradients (i_1 , i_2 , i_3), in each of the stages are summarized in Table 5 where the subscripts of 1, 2 and 3 correspond to the 1st, 2nd and 3rd stage of the test, respectively.

3.1.2. RWP test results on fully saturated GCL specimens

Four GCL specimens were prepared. Two were virgin specimens with no freeze–thaw cycles and two were specimens subjected to 5 freeze–thaw cycles. The bulk void ratio during water permeation and jet fuel permeation, was calculated when the hydraulic conductivity and GCL height had reached constant values (after at least one pore volume of flow). The virgin GCL specimens had lower bulk void ratios than the GCL specimens subjected to freeze–thaw cycles (Table 4). This indicates that the pore space in the bentonite increased due to the freeze–thaw cycles. However this did not appear to affect the hydraulic conductivity with respect to water which remained essentially the same after 5 freeze–thaw cycles. After permeation to equilibrium, the average total liquid (pore water and jet fuel) content (L) of the virgin GCL specimens was about 133% and that of the GCL specimens after freeze–thaw cycles was about 192% (see Table 4).

The hydraulic conductivity (k_1) of the GCL specimens with respect to de-aired water averaged about 2.0×10^{-11} m/s for both the specimens with no freeze–thaw and those with 5 freeze–thaw cycles once steady flow was reached (Table 5). Initial permeation by jet fuel (k_2) resulted in a reduction in the hydraulic conductivity of the GCL due to the difference between the density and viscosity of jet fuel compared to that of water. However, with time, interaction between the jet fuel and bentonite resulted in an increase in hydraulic conductivity (k_3). For the specimens with no freeze–thaw the final (equilibrium) hydraulic conductivity with respect to jet fuel was, within measurement accuracy, the same as the value with respect to water ($\approx 2.0 \times 10^{-11}$ m/s). For the specimens subjected to 5 freeze–thaw cycles, the average final equilibrium hydraulic conductivity with respect to jet fuel was about 8.0×10^{-11} m/s (i.e. about 4 times higher than the initial value with respect to water), but still low.

These tests were conducted at very high gradients (see Table 5) compared to the field and this raises a question regarding the effect of such high gradients on hydraulic

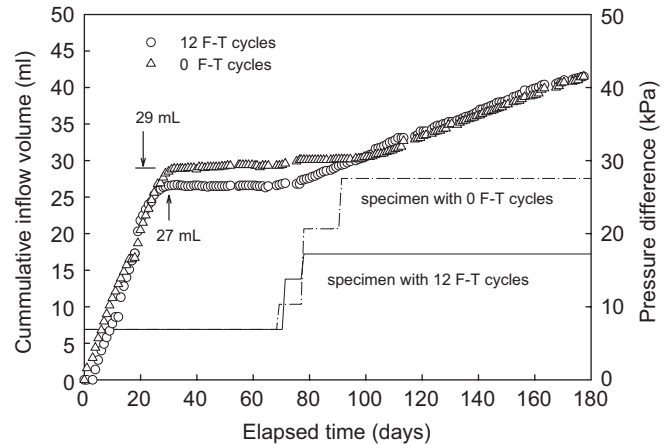


Fig. 2. Cumulative inflow volume through the GCL specimens subjected to 0 and 12 freeze–thaw cycles (F–T = freeze–thaw cycles).

conductivity. In an attempt to address this question a corresponding series of FWP tests was conducted.

3.1.3. FWP test results on fully saturated GCL specimens

Permeation of jet fuel causes the bentonite to shrink due to contraction of the double layer. However, it is difficult to measure the thickness of the GCL specimen during the hydraulic conductivity test using the flexible wall permeameter. To evaluate the hydraulic conductivity in each stage, the initial thickness of each specimen is used to calculate the hydraulic gradient in stage 1 while the hydraulic gradients in stages 2 and 3 are calculated based on the thickness of each GCL specimen after termination of the test. The pressure difference across all specimens was 7 kPa during the water permeation stage (i.e. in stage 1). Hydraulic conductivities for both specimens with 0 and 12 freeze–thaw cycles were $3.4\text{--}4.1 \times 10^{-11}$ m/s.

Fig. 2 shows the cumulative inflow volumes of GCL specimens subjected to 0 and 12 freeze–thaw cycles. At a fluid pressure of 7 kPa, the replacement of water by jet fuel as the permeant resulted in a reduction in the inflow rate to zero for both GCL specimens. The jet fuel could not permeate the GCL specimen because the fluid pressure was less than the threshold pressure required to overcome the interfacial tension between pore water and jet fuel. For the specimen subjected to 12 freeze–thaw cycles, bentonite had

worked its way into the geotextile during the freeze–thaw cycles and the surface of the geotextile became the initial barrier to jet fuel.

To establish the magnitude of the threshold pressure, the pressure head was increased in steps (and the cumulative volume monitored for 1 week) until flow restarted (Fig. 2). The threshold pressure was found to be between 21 and 28 kPa for the GCL specimen subjected to 0 freeze–thaw cycles and 14 and 18 kPa for the GCL specimen subjected to 12 freeze–thaw cycles. Hydraulic gradients calculated using the maximum threshold pressure are given in Table 5. The threshold hydraulic gradient for the GCL specimen subjected to 0 freeze–thaw cycles is about 2.4 times greater than that for the GCL specimen subjected to 12 freeze–thaw cycles. The difference in threshold pressure is attributed to the change in the void structure of the bentonite due to freeze–thaw cycles. However, in both cases, the threshold pressure is greater than the pressure differential likely to be encountered in the field application under consideration and thus no flow is anticipated in the field case (Bathurst et al., 2006).

The hydraulic conductivity with respect to jet fuel for the GCL specimen with 0 freeze–thaw cycles was about half that of the GCL specimen with 12 freeze–thaw cycles (see k_3 column in Table 5). However, both values are still low (less than 2×10^{-10} m/s). Hence, the GCL with 12 freeze–thaw cycles appears to be a suitable barrier to jet fuel in the short and medium term (certainly up to 4 years and potentially much longer). The elapsed times in these FWP tests until jet fuel appeared in the effluent (stage 3) were 273 days for the GCL specimen with 0 freeze–thaw cycles, and 340 days for the GCL specimen with 12 freeze–thaw cycles. To reduce FWP test times, a hydraulic gradient substantially higher than that expected in the field was used. Hence, the results reported here are considered likely to represent a worst case scenario because of the resistance provided by interface tension at the lower gradient in the field.

3.1.4. Evaluation of long-term barrier performance

Table 6 presents the intrinsic permeability values calculated from the data in Tables 2 and 5. Rowe et al. (2004b) reported that the intrinsic permeability did not

Table 6
Intrinsic permeability of GCL specimens with respect to both water and jet fuel

Test method	K_1^* (m ²)	K_2 (m ²)	K_3 (m ²)	K_3/K_1
RWP (0) ^a	2.1×10^{-18}	2.9×10^{-18}	6.9×10^{-18}	3.3
RWP (5) ^a	2.2×10^{-18}	2.0×10^{-18}	2.8×10^{-17}	12.7
FWP (0) ^a	5.3×10^{-18}	2.1×10^{-19}	3.3×10^{-18}	0.6
FWP (12) ^a	6.5×10^{-18}	1.2×10^{-18}	5.0×10^{-18}	0.8

* $K_1 = k_1 \eta / \gamma$, where k_1 is a hydraulic conductivity [LT⁻¹], η is a dynamic viscosity [ML⁻¹T⁻¹] at 20 °C and γ is unit weight [ML⁻²T⁻²].

^a() Number of freeze–thaw cycles.

change significantly due to permeation by jet fuel in the short to medium term. However, in the present tests, the permeation of at least 5 pore volumes of jet fuel resulted in a long-term (equilibrium) intrinsic permeability about a factor of three higher than that for water and, 0 freeze–thaw cycles, and a factor of 13 times higher for the specimens for water after 5 freeze–thaw cycles (Table 6). Rowe et al. (2004c) reported that jet fuel permeation resulted in a decrease in bulk void ratio but an increase in intrinsic permeability.

3.1.5. Hydraulic conductivity of unfrozen and frozen unsaturated GCL specimens

GCLs will quickly take up water from the adjacent soil that has an initial water content greater than 8–10% (Eberle and von Maubeuge, 1997). Hence, the GCL is likely to quickly achieve a degree of saturation, S_r , in excess of 60% under these circumstances and may be expected to have a degree of saturation in excess of 90% after 1–2 months (or even sooner for a foundation soil with a higher water content). Although the free water in a GCL is expected to freeze at about 0 °C, jet fuel does not freeze until about –47 °C and so one can anticipate potential permeation of jet fuel through an unsaturated GCL at subsurface temperatures of –5 to –20 °C. To examine the effect of the degree of saturation and temperature, GCL specimens with 2 different degrees of saturation were permeated with jet fuel at 4 temperatures (i.e. 20, 5, –5 and –20 °C). Using the constant head apparatus in a cold room at –5 °C, with a dry specimen (water content less than 8%) consolidated under 14 kPa, a preliminary upper bound on hydraulic conductivity was found to be 2.0×10^{-6} m/s. Fig. 3 shows hydraulic conductivity with respect to jet fuel at 20 °C for GCL specimens with different degrees of saturation between about 60% and 100%. The bulk void ratios of these GCLs ranged from 2.07–2.81 for S_r 58–65% and 2.2–3.0 for S_r 73–100%. The hydraulic conductivities for a degree of saturation $S_r = 60\%$ are given in Table 7.

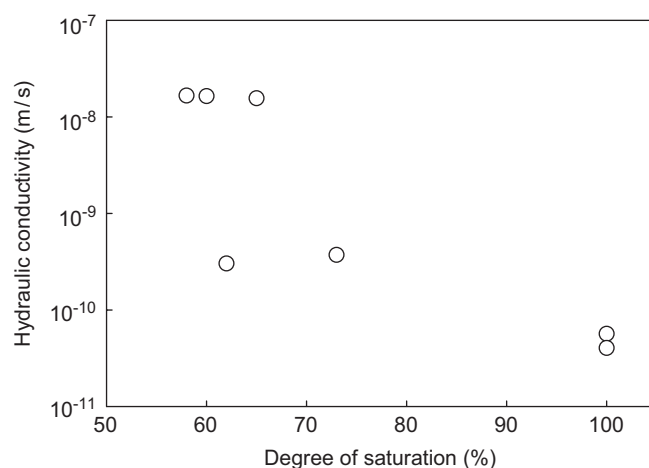


Fig. 3. Hydraulic conductivity (with respect to jet fuel) of GCLs different degrees of saturation at 20 °C.

The fact that the hydraulic conductivity for GCL specimens at $S_r = 90\%$ was higher at 5°C than that at 20°C , is suspected to be a result of variable distributions of water that can occur under unsaturated conditions. Except for this case, the hydraulic conductivity with respect to jet fuel decreased when temperature decreased. Since the density and viscosity of jet fuel are sensitive to temperature change it is desirable to examine the resistance to the flow of jet fuel in terms of the intrinsic permeability. Using a correlation between dynamic viscosity and temperature reported by Lewis and Squires (1934) and densities at each temperature obtained from Table 2, the calculated intrinsic permeability of a GCL and its variation with temperature is shown in Fig. 4 for unsaturated GCL specimens (i.e. $S_r = 60\%$ and 90%). The intrinsic permeability at $S_r = 90\%$ is typically less than at 60% and in both cases tends to decrease with temperature. In particular, the intrinsic permeability is smaller at temperatures below 0°C than for those above 0°C and this is attributed to a change in pore structure as the pore water freezes and expands. There is a further decrease in intrinsic permeability between -5 and -20°C . This is interesting since the effect of

temperature on viscosity and density have both been considered in the calculation of the intrinsic permeability and suggests that there is some additional change in the structure of the GCL between -5 and -20°C . More research is required to better understand this finding, although it may be hypothesized that this arises because some pore water did not freeze at -5°C but did freeze at -20°C . The decrease in intrinsic permeability with higher degree of saturation is to be expected. These results demonstrate that the degree of saturation of the GCL is an important factor to be considered when evaluating its likely performance as a barrier to jet fuel.

The forgoing results at -5°C were for specimens frozen prior to any permeation. Tests were also conducted on unsaturated specimens permeated with jet fuel at 5°C , frozen, and then re-permeated with jet fuel at -5°C (Table 8). In this case the intrinsic permeability did not change significantly with the change in temperature. It appears that the initial permeation by jet fuel did have some effect on the structure and reduced the effects of freezing on the closure of the main flow paths.

In summary, as might be expected, GCLs with low degree of saturation ($S_r = 60\%$) do not perform well as a barrier to jet fuel as GCLs with higher degrees of saturation (either frozen or unfrozen). Jet fuel was able to find flow paths through unsaturated but frozen GCLs at both $S_r = 60\%$ and 90% although lower temperature did appear to result in some structural change that decreased the intrinsic permeability. It may be hypothesized that this is due to the expansion of water as it freezes, decreasing the available pore space for jet fuel flow. The difference between the behaviour at -5 and -20°C may be due to a depression in the freezing point of water in small pores which prevented their freezing at -5°C but was not low enough to prevent freezing at -20°C . The permeation of jet fuel prior to freezing appears to have influenced the way the specimen eventually froze and freezing had much less effect in reducing the intrinsic permeability for these specimens than for specimens that were frozen prior to permeation. From a practical standpoint, these results suggest that freezing of unsaturated samples, while reducing the permeability, can not be relied upon to give low hydraulic conductivity and it is highly desirable to have the GCL fully hydrated prior to freezing and contact with jet fuel.

Table 7
Hydraulic conductivity of GCL specimens with respect to jet fuel at each temperature tested

Temperature ($^\circ\text{C}$)	Hydraulic conductivity of jet fuel (m/s)	
	Saturation degree ($S_r = 60\%$)	Saturation degree ($S_r = 90\%$)
20	1.6×10^{-8}	3.4×10^{-10}
5	1.6×10^{-9}	1.4×10^{-9}
-5	2.4×10^{-10}	9.0×10^{-11}
-20	2.8×10^{-11}	1.8×10^{-11}

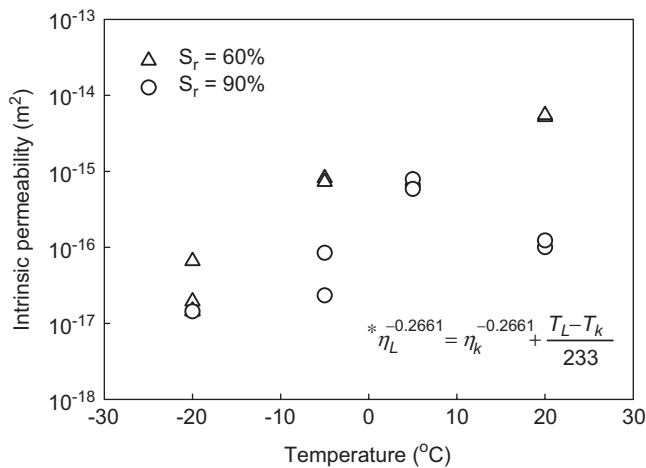


Fig. 4. Effect of temperature on intrinsic permeability of jet fuel on GCL specimens. *Equation obtained from Lewis and Squires (1934), η_L and η_k are the dynamic viscosities [MPa-s] at temperatures of T_L and T_k , respectively [$^\circ\text{K}$].

Table 8
Intrinsic permeability (K) of unsaturated GCL specimens permeated with jet fuel at 5°C and -5°C

Saturation degree (%)	e_B	K at 5°C (m^2)	K at -5°C (m^2)
61	2.3	7.2×10^{-16}	8.2×10^{-16}
63	2.1	7.7×10^{-16}	7.3×10^{-16}
90	2.3	7.9×10^{-16}	5.8×10^{-16}
95	2.7	5.9×10^{-16}	2.6×10^{-16}

3.2. Assessment of geomembrane properties

3.2.1. Tensile properties of geomembrane specimens immersed in jet fuel

Immersion in jet fuel for 18 weeks (at 23 °C) did not appear to result in any significant change in yield strength compared to the initial properties of the geomembrane (Fig. 5) and the initial drop is likely due to variability in the geomembrane properties rather than an effect of the jet fuel immersion. While fluorination of the geomembranes reduced the permeability of the geomembrane to hydrocarbons, this did not have a significant effect on the stress–strain behaviour upon immersion in jet fuel (i.e. strain at yield, and the breaking strength and strain did not change significantly). The data in Fig. 5 is consistent with data for samples retrieved from the Brevoort Island site that showed no indication of a systematic and significant change in the index tensile properties of the same f-HDPE geomembrane after 3 years of in-soil exposure to jet fuel contaminated ground (Bathurst et al., 2006).

3.2.2. OIT of the geomembrane

Fig. 6 shows the change in OIT values with respect to time for the geomembrane specimens immersed in jet fuel. At each sampling event at least three replicate specimens were tested and the vertical bars in Fig. 6 represent the standard deviation deduced from these tests. The OIT values decreased exponentially with immersion time. The initial OIT value of the untreated geomembrane was 135 min. This reduced to 70 min after 8 weeks, 22 min after 30 weeks and 8 min after 60 weeks of immersion in jet fuel. Between weeks 14 and 26, some scatter is observed in the data and the OIT values did not decrease at the same rate as was observed during the initial 14 weeks of immersion. It was hypothesized that diffusion of antioxidants from the geomembrane resulted in an increase in their concentration in the jet fuel adjacent to the geomembrane, thereby reducing the concentration gradient and the consequent

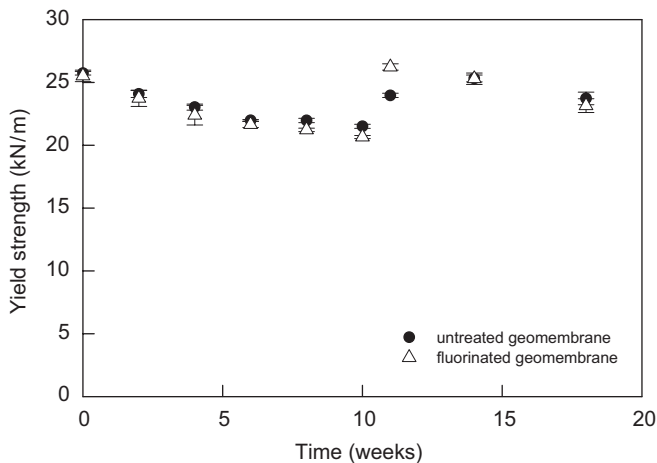


Fig. 5. Variation in yield strength with time of geomembrane exposure to jet fuel (error bars represent ± 1 standard deviation for test on 5 specimens).

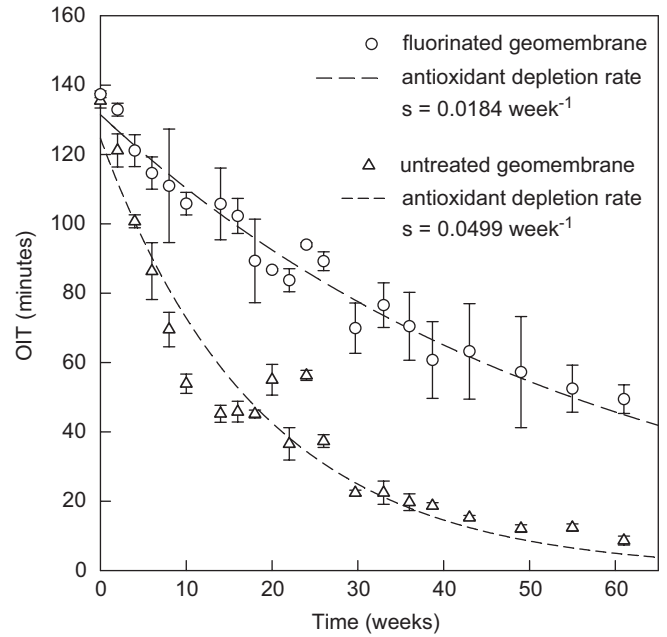


Fig. 6. Variation of standard OIT with immersion time for untreated and fluorinated geomembrane specimens. (error bars represent ± 1 standard deviation from three specimens).

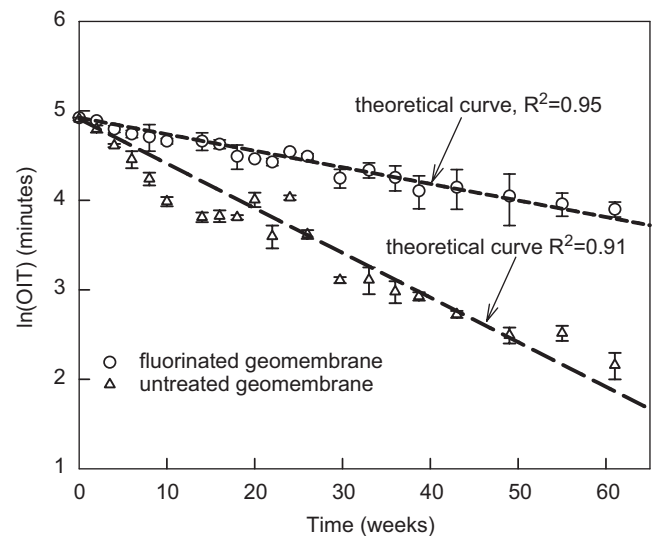


Fig. 7. Plot of $\ln(\text{OIT})$ with immersion time in jet fuel for untreated and fluorinated geomembrane specimens. (error bars represent ± 1 standard deviation from three specimens).

migration of antioxidants from geomembrane into the jet fuel. Having identified this potential concern on week 27, the jet fuel in the bath was completely replaced. After this replacement, a more rapid decrease in OIT value was observed, providing some support for the hypothesis. The antioxidants depletion rate was calculated using regression of $\ln(\text{OIT})$ values versus incubation time (Fig. 7). At any given immersion period the OIT value representing the total antioxidant amount in the geomembrane can be

expressed as

$$\text{OIT} = \text{OIT}_0 \exp(-s \times t), \quad (1)$$

where OIT_0 is initial OIT (in minutes); s is antioxidant depletion rate (in weeks⁻¹); and t is time (in weeks).

The antioxidant depletion rate of jet fuel-immersed untreated geomembrane was 0.2138 month⁻¹. This is 12.6 times faster than the depletion rate (0.0170 month⁻¹) for untreated 1.5 mm-thick HDPE geomembrane in synthetic municipal solid waste (MSW) leachate at 23 °C.

The initial OIT value of the fluorinated geomembrane was 137 min and this reduced to 111 min after 8 weeks, 70 min after 30 weeks, and 49 min after 60 weeks of immersion in jet fuel. The relationship between OIT and immersion time is exponential as shown in Fig. 6. The antioxidant depletion rate, s , was calculated to be 0.0788 month⁻¹ (Fig. 6). This is 2.7 times slower than the untreated geomembrane.

The time for complete antioxidant depletion at room temperature (~23 °C) was calculated, based on initial values of 135 min (for untreated geomembrane) and 137 min (for fluorinated geomembrane) and a residual OIT = 0.5 min (unstabilized HDPE), using Eq. (1). For the untreated geomembrane this was 112 weeks (2.2 years) while for the fluorinated geomembrane it was 305 weeks (5.9 years). The difference between the antioxidant depletion times for the untreated and fluorinated geomembranes was 193 weeks (3.7 years). Thus the results indicate that the fluorination had beneficial effect and increases the antioxidant depletion time of the geomembrane exposed to jet fuel. The antioxidant depletion times would be expected to be much longer at field temperatures in the Arctic, and so it can be inferred that the “service life” of the geomembrane will be in excess (and potentially very much in excess) of 6 years.

4. Conclusions

Questions have arisen regarding the likely service life of a geocomposite barrier installed in the Arctic to provide temporary containment of jet fuel. To assess the potential impacts of extreme climatic conditions and exposure to jet fuel, the hydraulic conductivity of saturated GCL specimens subjected to freeze–thaw cycles and unsaturated GCL specimens at different temperatures (including frozen conditions) was examined. Tests were performed using both flexible wall (FWP) and rigid wall (RWP) permeameters. In addition, the effect of exposure of both untreated and fluorinated HDPE geomembranes to jet fuel was investigated with respect to the yield strength and oxidative induction time. The results of these tests indicate that for the specific GCL and geomembranes and conditions examined:

- The hydraulic conductivity with respect to water was between 2.0×10^{-11} (RWP) and 3.4×10^{-11} m/s (FWP) at 14 kPa before freeze–thaw, and 2.0×10^{-11} (RWP) and 4.1×10^{-11} m/s (FWP) at 14 kPa after freeze–thaw.

- The long-term hydraulic conductivity of the GCL after the freeze–thaw cycles with respect to jet fuel was about 4 times greater than that for water, but was still very low. The intrinsic permeability of freeze–thaw specimens permeated with water, and then jet fuel was 2.2×10^{-18} m² and 2.8×10^{-17} m² (RWP) and 6.5×10^{-18} m² and 6.3×10^{-17} m² (FWP), respectively.
- GCLs with a low degree of saturation ($S_r = 60\%$) did not perform as well as an hydraulic barrier against jet fuel as specimens with higher (90% and 100%) degrees of saturation either before or after freezing. However, when frozen, the intrinsic permeability of the unsaturated GCLs dropped, with a greater effect at lower temperature (–20 °C) than at higher temperature (–5 °C), suggesting that there is some difference in the effect of temperature even for sub-freezing temperatures. However, if the GCL was permeated with jet fuel prior to freezing, freezing had very little effect on the intrinsic permeability.
- The tensile test results did not show any significant changes in yield strength of the geomembrane as a result of immersion in jet fuel for 18 weeks.
- Immersion in jet fuel substantially accelerates the antioxidant depletion rate relative to that observed in water or municipal solid waste (MSW) leachate. Fluorination of the HDPE geomembrane provided a significant beneficial effect and the antioxidants depleted at much higher rate (2.7 times faster) for the untreated geomembrane than for the fluorinated geomembrane. The total antioxidant depletion time was estimated to be 2.2 and 5.9 years for untreated and fluorinated geomembranes respectively at 23 °C and is expected to be much longer at field temperatures in the Arctic.

Based on these laboratory tests, it appears that the GCL used in the trial geocomposite barrier at Brevoort Island site can be expected to perform well as an hydraulic barrier in the short to medium term (at least up to 4 years and potentially much longer) with respect to the effect of both freeze–thaw and permeation with jet fuel. The results also demonstrate the beneficial effect of fluorination of HDPE geomembrane used at the site. The service life is expected to be considerably greater than 6 years.

Acknowledgements

The barrier system at Brevoort Island (BAF-3) was constructed on behalf of the North Warning System Office, Department of National Defence, Canada. Their support throughout the project is gratefully acknowledged. The writers are also indebted to Dr. Barbara Zeeb, Dr. Ken Reimer, and Dr. Chris Ollson of the Environmental Sciences Group (ESG) at RMC. Additional funding for laboratory studies of GCLs was provided by CRESTech, an Ontario centre of excellence, and Terrafix Geosynthetics Inc. The value of discussions with Mr. K. Von Mauberge and B. Herlin is gratefully acknowledged.

References

- ASTM, 1992. D5261, Standard Test Method for Measuring Mass per Unit Area of Geotextiles. The American Society for Testing and Materials, vol. 4.09, pp. 1310–1311.
- ASTM, 1996. D5993-96, Standard Test Method for Measuring the Mass per Unit Area of GCL. The American Society for Testing and Materials, vol. 4.09, pp. 1426–427.
- ASTM, 1997. D5084-90, Standard Test Method for Measurement of Hydraulic Conductivity of Saturated Porous Materials Using a Flexible Wall Permeameter. The American Society for Testing and Materials, vol. 4.09, pp. 62–69.
- ASTM, 1997. D6035-96, Standard Test Method for Determining the Effect of Freeze–thaw on Hydraulic Conductivity of Compacted or Undisturbed Soil Specimens Using a Flexible Wall Permeameter. The American Society for Testing and Materials, vol. 5.01, pp. 1004–1007.
- ASTM, 1998a. D638-97, Standard Test Method for Tensile Properties of Plastics. The American Society for Testing and Materials. vol. 8.01 Plastics (I), pp. 46–58.
- ASTM, 1998b. D1480-91, Standard Test Method for Density and Relative Density (Specific Gravity) of Viscous Materials by Bingham Pycnometer. The American Society for Testing and Materials, vol. 5.01, pp. 539–544.
- ASTM, 1998c. D3895-97, Standard Test Method for Oxidative Induction Time of Polyolefins by Differential Scanning Calorimetry. The American Society for Testing and Materials, vol. 8.02 Plastics (II), pp. 486–491.
- ASTM, 1998d. E794-95, Standard Test Method for Melting and Crystallization Temperatures by Thermal Analysis. The American Society for Testing and Materials, vol. 14.02 General Test Methods; Nonmetals; Chromatography; Durability of Nonmetallic Materials; Forensic Sciences; Laboratory Apparatus; Statistical Methods, pp. 483–486.
- ASTM, 2003. D6693-01, Standard Test Method for Determining Tensile Properties of Nonreinforced Polyethylene and Nonreinforced Flexible Polypropylene Geomembranes. The American Society for Testing and Materials, vol. 04.13 Geosynthetics, pp. 392–395.
- ASTM, 2002. D6766-02, Standard Test Method for Evaluation of Hydraulic Properties of Geosynthetic Clay Liners Permeated with Potentially Incompatible Liquids. The American Society for Testing and Materials, vol. 10.03 Electrical Insulating Liquids and Gases, pp. 415–423.
- Barroso, M., Touze-Foltz, N., von Maubeuge, K., Pierson, P., 2006. Laboratory investigation of flow rate through composite liners consisting of a geomembrane, a GCL and a soil liner. *Geotextiles and Geomembranes* 24 (3), 139–155.
- Bathurst, R.J., Rowe, R.K., Zeeb, B., Reimer, K., 2006. A geocomposite barrier for hydrocarbon containment in the Arctic. *International Journal of GeoEngineering Case Histories* 1 (1), 18–34.
- Bouazza, A., Vangpaisal, T., 2006. Laboratory investigation of gas leakage rate through a GM/GCL composite liner due to a circular defect in the geomembrane. *Geotextiles and Geomembranes* 24 (2), 110–115.
- Cartaud, F., Touze-Foltz, N., Duval, Y., 2005a. Experimental investigation of the influence of a geotextile beneath the geomembrane in a composite liner on the leakage through a hole in the geomembrane. *Geotextiles and Geomembranes* 23 (2), 117–143.
- Cartaud, F., Goblet, P., Touze-Foltz, N., 2005b. Numerical simulation of the flow in the interface of a composite bottom liner. *Geotextiles and Geomembranes* 23 (6), 513–533.
- CHEM INFO—Canadian Centre for Occupational Health and Safety Issue: 2001–2.
- Dickinson, S., Brachman, R.W.I., 2006. Deformations of a geosynthetic clay liner beneath a geomembrane wrinkle and coarse gravel. *Geotextiles and Geomembranes* 24 (5), 285–298.
- Eberle, M.A., von Maubeuge, K., 1997. Measuring the in-situ moisture content of geosynthetic clay liners (GCLs) using time domain reflectometry (TDR). In: *Proceedings of Sixth International Conference on Geosynthetics*, Atlanta, Industrial Fabrics Association International, vol. 1, pp. 205–210.
- Elert, G., 2003. *The Physics Hypertextbook*TM, <<http://hypertextbook.com/physics/>>.
- Fernandez, F., Quigley, R.M., 1985. Hydraulic conductivity of natural clays permeated with simple liquid hydrocarbons. *Canadian Geotechnical Journal* 22, 205–214.
- Hsuan, Y.G., Koerner, R.M., 1995. Long term durability of HDPE geomembrane: part I—depletion of antioxidant. GRI Report, Geosynthetic Research Institute, Drexel University, Philadelphia, PA, pp. 16–35.
- Hsuan, Y.G., Koerner, R.M., 1998. Antioxidant depletion lifetime in high density polyethylene geomembranes. *Journal of Geotechnical and Geoenvironmental Engineering ASCE* 124 (6), 532–541.
- Koerner, R.M., Lord, A.E., Hsuan, Y.H., 1992. Arrhenius modelling to predict geosynthetics degradation. *Geotextiles and Geomembranes* 11, 151–183.
- Lake, C.B., Rowe, R.K., 2005. A comparative assessment of volatile organic compound (VOC) sorption to various types of potential GCL bentonites. *Geotextiles and Geomembranes* 23 (4), 323–347.
- Lewis, W.K., Squires, L., 1934. *Refiner Nat. Gasoline Manuf* 13 (12), 448.
- Li, H.M., Bathurst, R.J., Rowe, R.K., 2002. Use of GCLs to control migration of hydrocarbons in severe environmental conditions. In: *International Symposium on Geosynthetic Clay Barriers*, Nuremberg, Germany, April, pp. 187–198.
- Mukunoki, T., Rowe, R.K., Li, M.H., Sangam, H.P., Hurst, P., Badv, K., Bathurst, R.J., 2003. Hydraulic conductivity and diffusion characterization of GCLs. In: *Proceedings of the 56th Canadian Geotechnical Conference and Fourth Joint IAHC-CNC/CGS 2003 NAGS Conference*, pp. 668–674.
- Müller, W., Jakob, I., 2003. Oxidative resistance of high-density polyethylene geomembranes. *Polymer Degradation and Stability* 79, 161–172.
- Petrov, R.J., Rowe, R.K., 1997. Geosynthetic clay liner (GCL)—chemical compatibility by hydraulic conductivity testing and factors impacting its performance. *Canadian Geotechnical Journal* 34, 863–885.
- Petrov, R.J., Rowe, R.K., Quigley, R.M., 1997. Comparison of laboratory measured GCL hydraulic conductivity based on three permeameter types, *American Society for Testing and Materials. Geotechnical Testing Journal* 20 (1), 49–62.
- Rowe, R.K., 2005. Long-term performance of contaminant barrier systems⁷, 45th Rankine Lecture. *Geotechnique* 55 (9), 631–678.
- Rowe, R.K., Orsini, C., 2003. Effect of GCL and subgrade type on internal erosion in GCLs. *Geotextiles and Geomembranes* 21 (1), 1–24.
- Rowe, R.K., Quigley, R.M., Brachman, R.W.I., Booker, J.R., 2004a. *Barrier Systems for Waste Disposal Facilities*. Taylor & Francis Books Ltd (E & FN Spon), London, 587p.
- Rowe, R.K., Mukunoki, T., Li, M.H., Bathurst, R.J., 2004b. Effect of freeze–thaw on the permeation of arctic diesel through a GCL. *Journal of ASTM International* 1 (2), 1–13.
- Rowe, R.K., Mukunoki, T., Bathurst, R.J., 2004c. Compatibility of Arctic diesel through GCL with freeze and thaw. In: *Geosynthetics Conference Euro Geo 3*, Munich, Germany, March, pp. 193–196.
- Rowe, R.K., Hurst, P., Mukunoki, T., 2005a. Permeating partially hydrated GCLs with jet fuel at temperatures from –20 °C and 20 °C. *Geosynthetics International* 12 (6), 333–343.
- Rowe, R.K., Mukunoki, T., Bathurst, R.J., Rimal, S., Hurst, P., Hansen, S., 2005b. The performance of a composite liner for retaining hydrocarbons under extreme environmental conditions. In: *Proceedings of ASCE Geo-Frontiers 2005*, Austin, TX, 24–26 January 2005, 15p.
- Sangam, H.P., Rowe, R.K., 2002. Effects of exposure conditions on the depletion of antioxidants from high-density polyethylene (HDPE) geomembranes. *Canadian Geotechnical Journal* 39, 1221–1230.
- Touze-Foltz, N., Duquennoi, C., Gaget, E., 2006. Hydraulic and mechanical behavior of GCLs in contact with leachate as part of a composite liner. *Geotextiles and Geomembranes* 24 (3), 188–197.